THREE-DIMENSIONAL FE SOLID RESPONSE ANALYSIS OF RC COLUMNS SUBJECTED TO A COMBINATION OF PERMANENT ECCENTRIC AXIAL FORCE AND REVERCED CYCLIC TORSION AND BENDING/SHEAR

(Translation from Proceedings of JSCE, No.683/V-52, August 2001)



Satoshi TSUCHIYA Kazuhiro TSUNO Koichi MAEKAWA

The response behavior of RC solid columns subjected to a combination of a permanent eccentric axial force, reversed cyclic torsion and bending/shear force is investigated using nonlinear full 3D FE analysis in order to verify three-dimensional constitutive models that take into account non-orthogonal multi-directional cracking. It is verified that this analytical method can simulate the development of multi-directional cracks in three-dimensional space, and that modeling of spalling and buckling under torsion, bending and shear are important in the highly inelastic range. A primitive analysis covering large deformations of the main reinforcement is also implemented, and their overall effect on structural response is investigated. A visual representation of the situation in which the predominant three-dimensional variable inclined cracks change from step to step is possible using this analysis.

Keywords: *full 3D FE solid analysis, RC column members, cyclic torsion, cyclic horizontal force, permanent eccentric axial force, buckling behavior*

Satoshi Tsuchiya is a manager of COMS Engineering, Japan. He obtained his D. Eng. from the University of Tokyo in 2001. His research interests cover the seismic performance evaluation and numerical simulation of reinforced concrete structures.

Kazuhiro Tsuno is the chief engineer of the Metropolitan Expressway Public Corporation, Japan. He graduated from the Waseda University with a M.E. degree in the civil engineering in 1990 and received another M.E. from the University of Canterbury in New Zealand, in 2000. He has been involved in some bridge and tunnel projects, and a CALS project.

Koichi Maekawa is a professor in the Department of Civil Engineering at the University of Tokyo, Japan. He earned his D. Eng. from the University of Tokyo in 1985. The structural mechanics and constitutive laws for reinforced concrete have been investigated as his academic major background. He joined the project for development of self-compacting concrete in 1985-1989. After innovation of its prototype, he has been engaged in the project for micro-structural development of cementitious materials and computational durability assessment.

1. INTRODUCTION

In Japan's crowded areas, it is sometimes necessary to construct reinforced concrete highway piers in the shape of an inverted "L" or "T" to comply with space limitations. Since such piers are subjected to an axial load that is eccentric in the transverse direction, an important part of earthquake-resistant design is ensuring their structural safety under permanent eccentric axial forces. In order to clarify the seismic performance of structures with this kind of shape, the interactions among bending/shear forces derived from inertial force (the main action), the permanent eccentric axial force and additional torsion caused by the eccentric force (the secondary action) must be taken into account appropriately. Further, it needs to be shown that the external force acts through an arbitrary repeated loading path at performance verification stage from now on, as performance-based design method is introduced.

A number of experimental and analytical studies of RC members subjected to pure torsion or a combination of torsion and bending/shear have been reported, including [1][2] for example. However, the direction of principal stress in these target structures does not generally change very much, and many of the induced crack groups are perpendicular.

On the other hand, the path-dependency of RC plate elements with multi-directional cracks, more than three, has been approximately established. A full three-dimensional nonlinear structural analysis method [3] introducing the knowledge on the path-dependency as constitutive equations is being developed, and attempts have been made to enhance its applicability (for structural dimensions and loading path etc.). Although calculation efficiency is lower than when using beam-column frame elements or plate shell elements since there is no degeneration of the degrees of freedom (D.O.F.), the reliability of this new simulation method is gradually being improved through multilateral verification and improvement [4][5][6]. This analytical method enables us to quantitatively evaluate stress paths and damage distribution within a structure, which is not possible with loading tests. There are also expectations that the new method will make it possible to clarify the mechanism by which a structure resists multi-directional loading and to improve the design equation. For the authors, the establishment of full three-dimensional dynamic nonlinear solid analysis that does not require D.O.F degeneration is the long-term aim. They are moving forward with their work on the assumption that the analytical environment will become even richer in the near future. In this study, the aim is to verify the constitutive models for non-orthogonal multi-directional cracking, one key part of the analytical method, in a three-dimensional stress field.

An experiment on RC box-type hollow columns subjected to reversed cyclic torsion and bending/shear has already been simulated using plate shell elements with D.O.F. degeneration [7]. While plate shell analysis allows for reduced D.O.F. compared with solid analysis, assumptions relating to out-of-plane deformation and rotational limits must be introduced. Although the issue of cover concrete spalling due to torsion and degradation of torsional stiffness after buckling were left open in this work, the response torsional stiffness and bending/shear up to the ultimate state were accurately predicted.

As regards full three-dimensional analysis [5], experiments on RC columns subjected to pure torsion and multi-directional shear forces have been simulated with good results. Loading experiments on RC columns retrofitted with steel jackets and carbon fiber sheeting have also been investigated, and the analysis verified that ductility was improved. However, these simulations were for monotonic loading only, and the crack distribution was limited to one direction or two orthogonal directions. Consequently, they verify only one limited part of the constitutive models for three-dimensional non-orthogonal multi-directional cracking. It is premature to judge the propriety of the models from these results.

In this paper, the focus is an earlier loading experiment in which RC solid columns were subjected to a combination of a permanent eccentric axial force, reversed cyclic torsion and bending/shear force [8][9]. This experiment is made the target for verification of the non-orthogonal multi-directional cracking mechanical model, and full three-dimensional solid analysis is applied. The original aim of the experiment was to examine the influence of interactions among the eccentric axial force, bending/shear and torque on the seismic performance of RC columns. The investigation suggested that spalling of the cover concrete and buckling of the main reinforcing bars would have a non-negligible effect on overall deformational behavior. On the basis of a previous study [10][17][18], a simplified steel buckling model is introduced into the full three-dimensional solid analysis procedure, and the influence on overall response behavior is investigated.

An RC column under multi-axial stress and subjected to reversed cyclic torsion and bending/shear develops cracks in at least three directions. Accordingly, such a column is suitable for use in verifying the path-dependent multi-directional fixed smeared crack model [3][4]. In doing this, it is not possible to apply an analytical model that requires D.O.F. degeneration, so full three-dimensional solid analysis that takes into consideration the loading path is essential. Applying three-dimensional nonlinear frame analysis based on a fiber technique simplified out-of-plane deformation needs some transaction equivalent to a full three-dimensional approach from a view of engineering.

For a column subjected to a permanent eccentric axial force and reversed cyclic bending/shear only, frame analysis based on a fiber technique can be used because multi-axial bending is prominent [11]. Then, by comparing the analytical results obtained by frame analysis with D.O.F. degeneration and by full solid analysis, the accuracy and applicable range of frame analysis are discussed for a specimen without torsion.

Following the example of a previous study [11] of this subject, the "eccentric moment" is defined in this paper as the moment due to eccentric axial forces, and the "direction of eccentricity" as the orientation of the eccentric moment. Generally, the direction of eccentricity accords with the transverse axis.

2. SUMMAY OF PREVIOUS EXPERIMENTAL STUDY [8][9]

As already mentioned, the verification described here is based on a previous experiment. An outline of that experiment is given here.

2.1 Specimen and loading method

An actual RC pier with a comparatively large permanent eccentric moment is selected as the model, and scaled-down specimens (about 1/5 scale) are the targets of the study. The ratios of cover thickness and bar diameter to cross section are matched as closely as possible by considering the embedded length of the reinforcing bars and concrete compactability, etc. The dimensions and cross section are shown in Fig. 1, and material properties are given in Table 1.

There are three experimental specimens, numbered 1 to 3. Reversed cyclic torsion and eccentric axial force are set up as the experimental parameters, and reversed cyclic bending/shear is applied in the combinations indicated in Table 2. A vertical load of 245 (kN) is applied at the center of the cross section of column specimen 1, while a constant eccentric axial force of 147 (kN) is applied at a position 700 (mm) away from the center of the cross section for specimens 2 and 3. These values of eccentricity are determined such that the tensile stress on the reinforcing bars due to the eccentric moment is less than 1,200 (kgf/cm^2) or 117.6 (MPa). Bending cracks occur at the base of the column as a result of the eccentric moment. Reversed cyclic torsion and bending/shear are applied as follows (and as illustrated in Fig. 2):

1) Torsion is applied by displacement control using two oil-operated jacks at the original position of horizontal displacement (+ direction).
2) Bending/shear is applied up to +n δ_y while maintaining the torsional angle.
3) After return to the original position, torsion is applied in the reverse direction (- direction).
4) Similarly, bending/shear is applied up to –n δ_y and then the original state is restored.
5) Procedures 1) to 4) are repeated.

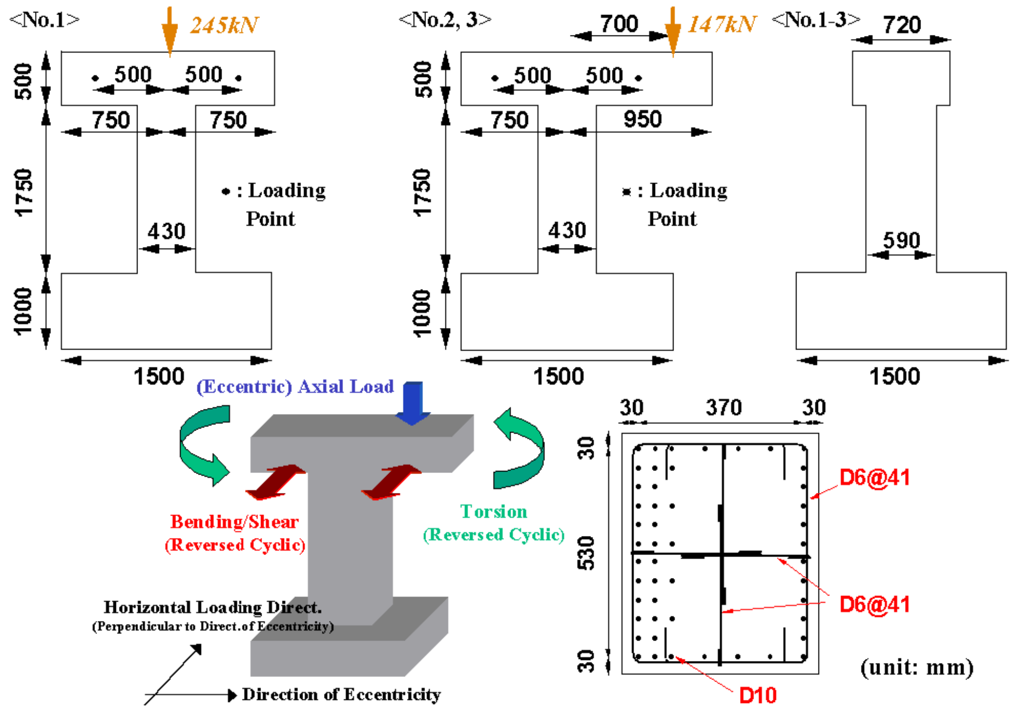

Fig. 1 Summary of Experimental Specimen

Table 1 Material Properties

		No.1	No.2	No.3
Concrete	Compressive Strength (MPa)	34.4	34.8	36.9
	Young's Modulus (*10^4MPa)	2.68	2.32	2.53
	Tensile Strength (MPa)	2.75	3.05	3.33
	Poisson's Ratio	0.161	0.189	0.164
D10	Yielding Strength (MPa)	402	393	393
	Young's Modulus (*10^5MPa)	1.87	1.88	1.88
D6	Yielding Strength (MPa)	384	384	384
	Young's Modulus (*10^5MPa)	1.83	1.92	1.92

Table 2 Combinations of Loading Methods

	No.1	No.2	No.3
Eccentric Axial Force	No (center of area)	Yes	Yes
Cyclic Torsion	Torsional Cracking	Torsional Yielding	No
Cyclic Bending / Shear	$\pm 9\delta_y$ (2cycles)	$\pm 6\delta_y$ (2cycles)	$\pm 7\delta_y$ (2cycles)

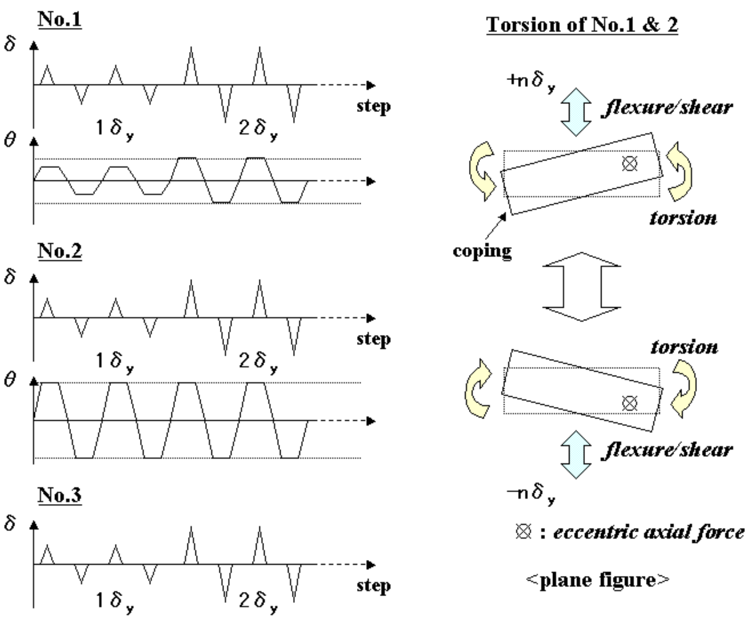

No.1
$+\delta_y = +9.9$mm, $-\delta_y = -9.0$mm
θ: torsional cracking rotational angle
(after $2\delta_y$, equal torque angle)
\# difference in jack displacement=±2.5mm
(only $1\delta_y$; 1.6mm)

No.2
$+\delta_y = +8.0$mm, $-\delta_y = -8.0$mm
θ: torsional yeilding rotational angle
\# difference in jack displacement=±15mm

No.3
$+\delta_y = +8.0$mm, $-\delta_y = -8.0$mm

Fig. 2 Loading Method

By checking the real-time response behavior during the loading test, the relative displacement due to torsion is decided as according with the torsional cracking moment for specimen 1 and torsional yielding moment for specimen 2 (see Fig. 2). Displacement values of the jacks are ±2.5 (mm) for specimen 1 except ±1 δ_y and ±15.0 (mm) for specimen 2, respectively. For the ±1 δ_y state of specimen 1, the value is ±1.6 (mm) [8]. For all specimens, the major portion of deformation is governed by flexure. However, three-directional cracking is at least introduced, namely in the form of diagonal cracks by torsion and shear and horizontal cracks by bending, when specimen 1 and 2 are subjected to reversed cyclic torsion, and the prominent deformation orientation changes cycle-by-cycle. Moreover, because the torque applied is considerable, and as high as the torsional yield value for specimen 2, its influence is not negligible.

2.2 Experimental results

a) Specimen 1
The relationship between load and displacement in the horizontal loading direction is shown in Fig. 3, and the relationship between torsional force (difference between the reaction forces of the two jacks) and displacement in Fig. 4. Concrete spalling begins in the compression zone as a result of bending at approximately 5 δ_y, reinforcing bar rupture is observed at 8 δ_y, and finally loading is terminated at the first 9 δ_y cycle. The crack distribution and damage after loading are shown in Fig. 5 and Photo 1. In addition to the rupture of the main reinforcing bars, there is some observational evidence of a buckling phenomenon.

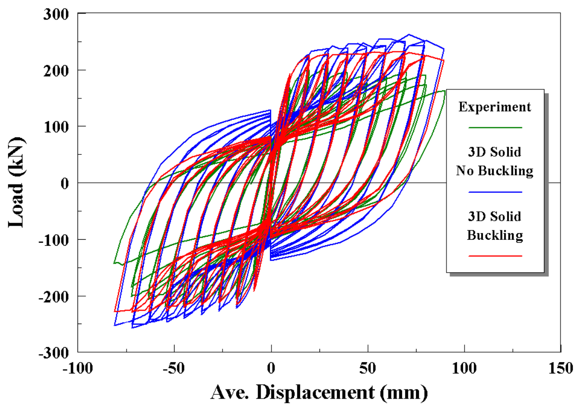

Fig. 3 Specimen 1 Load - Displacement Relationship in Horizontal Loading Direction

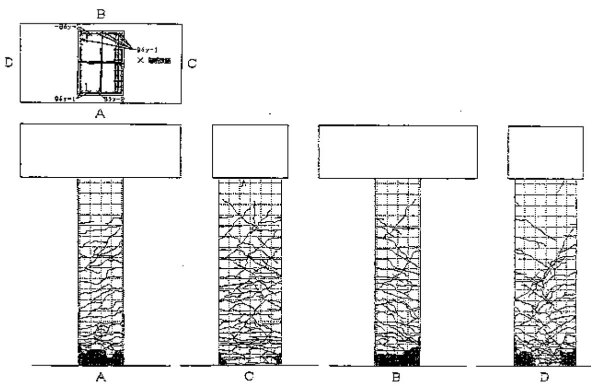

Fig. 5 Specimen 1 Crack Distribution after Loading

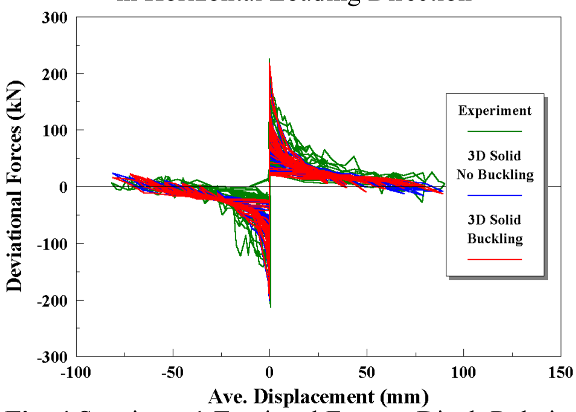

Fig. 4 Specimen 1 Torsional Force – Displ. Relationship


Photo 1 Specimen 1 Damage at Base

b) Specimen 2
As with specimen 1, the relationship between load and displacement in the horizontal loading direction is shown (Fig. 6) along with the relationship between torsional force and displacement (Fig. 7). Further, the relationship between displacement in the direction of eccentricity and that in the horizontal loading

direction is shown in Fig. 8. It is observed that a significant residual deformation accumulates in the direction of eccentricity (which is perpendicular to the horizontal loading direction; see Fig. 8 and Photo 2). Moreover, this residual displacement is larger than the applied displacement in the primary loading direction. Because this accumulated eccentric deformation exceeds the capacity of the experimental equipment, loading is terminated. Ultimately, the deformation reaches 140 (mm) and the rotational angle exceeds 1/20. Concrete damage due to the eccentric moment in the compression zone becomes significant from approximately 4 δ_y onward, and crushing occurs at 5 δ_y. The crack distribution at the first 6 δ_y cycle is illustrated in Fig. 9, and the post-loading damage is shown in Photo 3. Although no obvious symptoms of buckling are seen, continuity between concrete and reinforcing bars has been lost due to spalling.

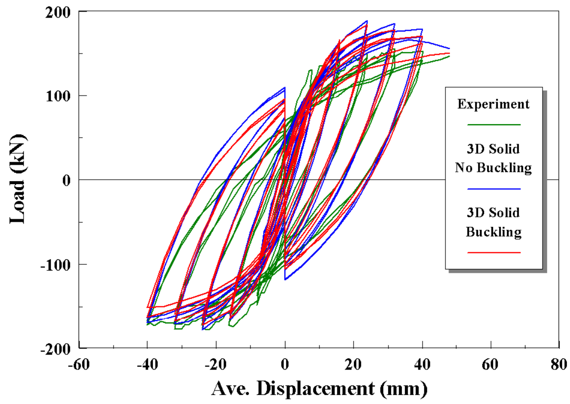

Fig. 6 Specimen 2 Load - Displacement Relationship in Horizontal Loading Direction

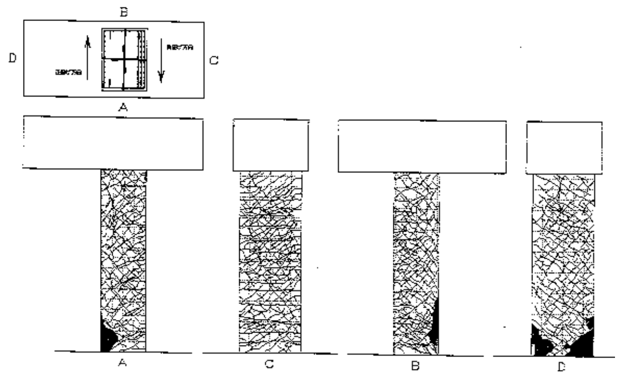

Fig. 9 Specimen 2 Crack Distribution after Loading

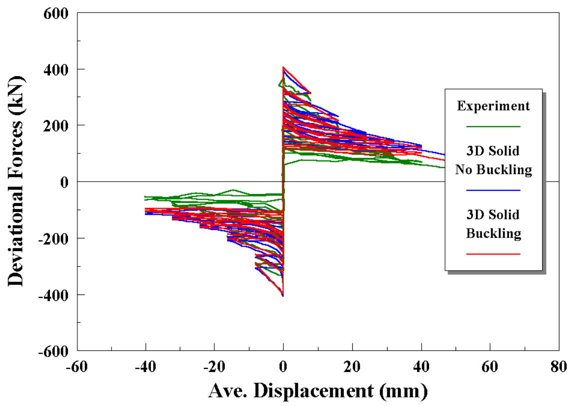

Fig. 7 Specimen 2 Torsional Force – Displ. Relationship

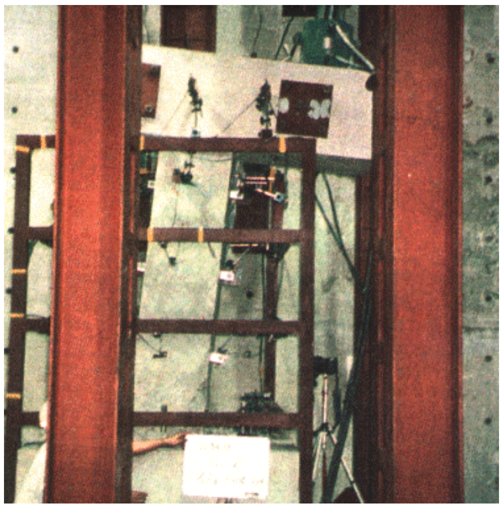

Photo 2 Specimen2 Deformation in Direction of Eccentricity

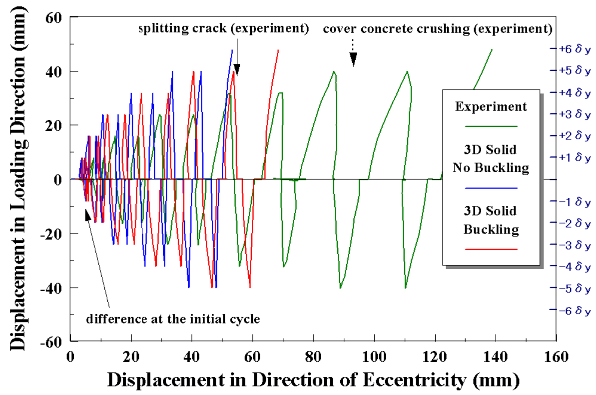

Fig. 8 Specimen 2 Displ. in Direction of Eccentricity -Displ. in Horizontal Loading Direction Relationship

Photo 3 Specimen 2 Damage at Base

c) Specimen 3

The relationship between load and displacement in the horizontal loading direction is shown in Fig. 10, and the relationship between displacement in the direction of eccentricity and that in the horizontal loading direction is shown in Fig. 11. It is observed that significant residual deformation accumulates in the direction of eccentricity even in this case, in which no torsion is applied (Fig. 11 and Photo 4). As with specimen 2, loading is terminated because the accumulated deformation in the direction of eccentricity exceeds the capacity of the experimental equipment. At this ultimate value state, the displacement reaches 120 (mm). Concrete damage due to the eccentric moment becomes significant in the compression zone from approximately 5 δ_y, and crushing occurs at 6 - 7 δ_y. The crack distribution at the first 7 δ_y cycle is illustrated in Fig. 12, and the post-loading damage is shown in Photo 5. Although no obvious symptoms of buckling are seen, continuity between concrete and reinforcing bars has been lost due to spalling.

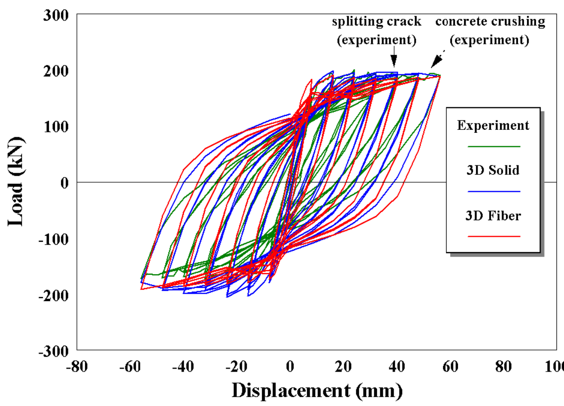

Fig. 10 Specimen 3 Load – Displ. Relationship in Horizontal Loading Direction

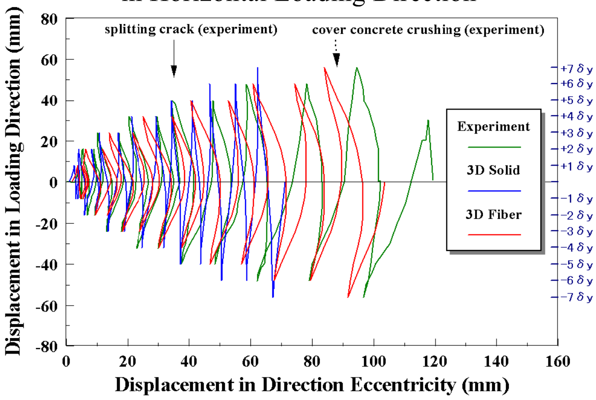

Fig. 11 Specimen 3 Displ. in Direction of Eccentricity -Displ. in Horizontal Loading Direction Relationship

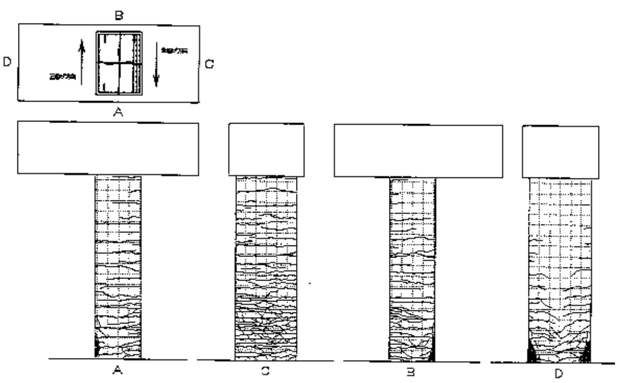

Fig. 12 Specimen 3 Crack Distribution after Loading

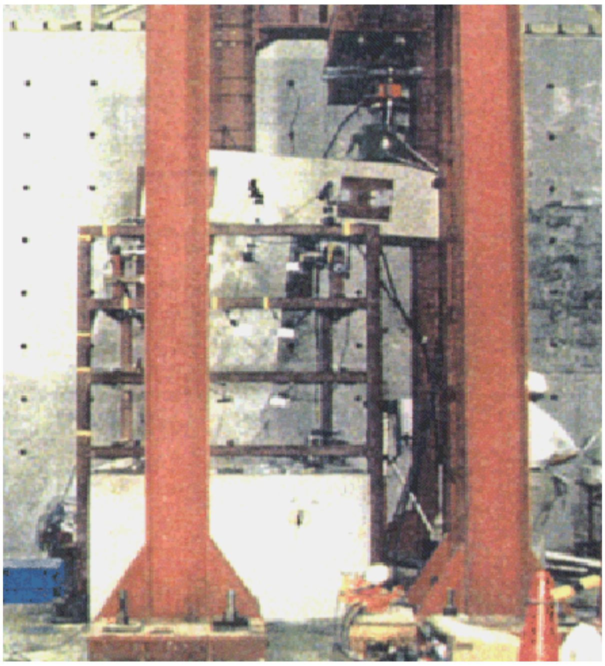

Photo 4 Specimen 3 Deformation in Direction of Eccentricity [11]

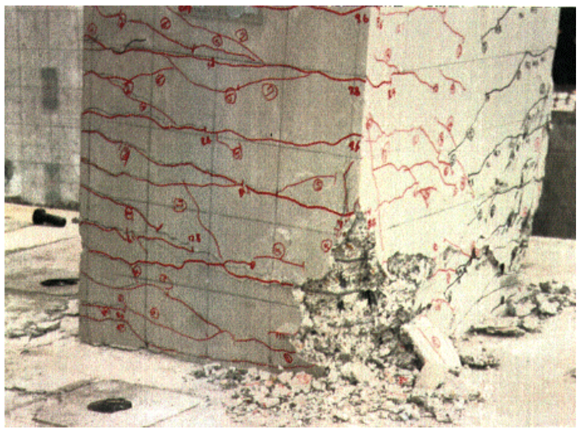

Photo 5 Specimen 3 Damage at Base [11]

3. FULL THREE DIMENSIONAL FE NONLINEAR ANALYSIS

3.1 Outline of analytical method

A method of full three-dimensional nonlinear solid analysis is established by extending RC plate models based on path-dependent material constitutive models [12] to three dimensions [5]. In the plain stress field, a multi-direction fixed crack model that can consider non-orthogonal cracking in up to four directions is adopted [3]. As regards interactions between superposed cracks, an active crack method is introduced in which nonlinear behavior related to the widest crack (the active crack) mainly governs the overall response. By considering opening/closing, slip and their interactions for cracks in all directions, a basis for calculating stress transfer has been established for an arbitrary loading path. In extending the two-dimensional RC plate models to three dimensions, the principal axis (1) is defined as the normal to the first cracking plane. Axes (2) and (3) are automatically determined from this first cracking plane, and sub-planes defined in terms of axes (1, 2), (2, 3) and (3, 1) are introduced as shown in Fig. 13. By applying the two-dimensional RC plate constitutive models to these three sub-planes, calculated transferred stresses are summarized for a representation of the three-dimensional stress field. Here, as a result of assuming that the rotational stress tensor is zero, it is possible to consider the interactions among nine non-orthogonal crack planes in three-dimensional space.

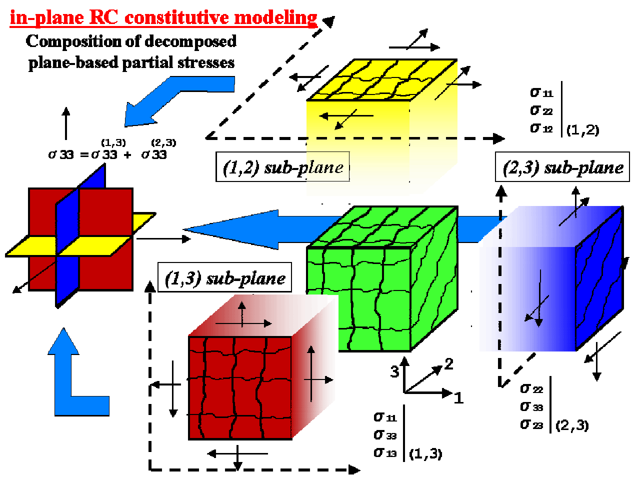

Fig. 13 Stress Computation Method for Three-Dimensional Solid Element [5]

In order to obtain accurate analytical results using relatively large elements, a zoning method is introduced for the three orthogonal directions. This entails dividing RC members into a bond area (RC zone) under the influence of reinforcing bars and a non-bond area (plain concrete zone) [13]. The analytical mesh is defined according to the arrangement of reinforcing bars, and tension stiffening is considered in the RC zone. For the plain concrete zone, the stress release rate is determined from the tensile fracture energy G_f and element length as satisfying the required fracture mechanics conditions.

In frame analysis based on the fiber technique, the sectional forces and moments are calculated from average axial strain and curvatures in two directions according to Euler's assumption, which states that a plane section remains plane. Material constitutive models applied to in-plane deformational behavior are the same as for full solid analysis. By simplifying the out-of-plane behavior as linear, D.O.F. are greatly reduced [11]. While this is very effective for RC columns in which flexural deformation is prominent, it should be noted that shear deformation would be underestimated.

Experimental measurements have demonstrated that horizontal displacement due to pull-out of reinforcing bars from the footing is not very significant, and reports suggest that the ratio to total displacement value is appropriately 15 (%) [14]. This is because the dimensions of the experimental specimen correspond as closely to those of a full-scale structure as possible. Therefore, pull-out is not considered in the analysis used here.

The analytical meshes are illustrated in Fig. 14. For the base of the column, where damage is concentrated, a small element length is defined in the axial direction so as to maintain analytical accuracy. In the cross section, a small length is defined near the surface of the column and a relatively large one inside because the torsional shear path is concentrated at the surface and compression is also concentrated there due to two-axis bending. Conversely, a relatively coarse element definition at the core part may not lead to deterioration of analytical accuracy because bending cracks are distributed within the column and little contribution to stress transfer is expected.

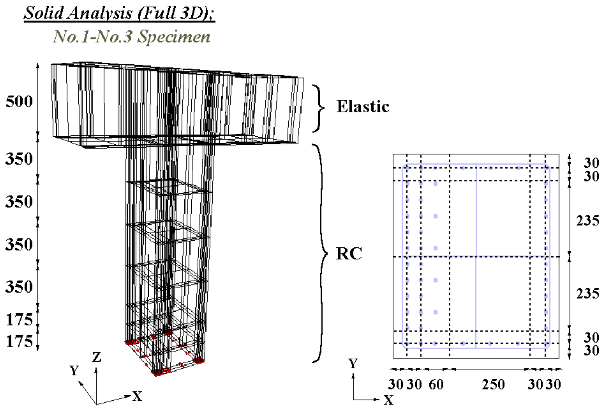

Fig. 14-1 Mesh Definition for Solid Analysis

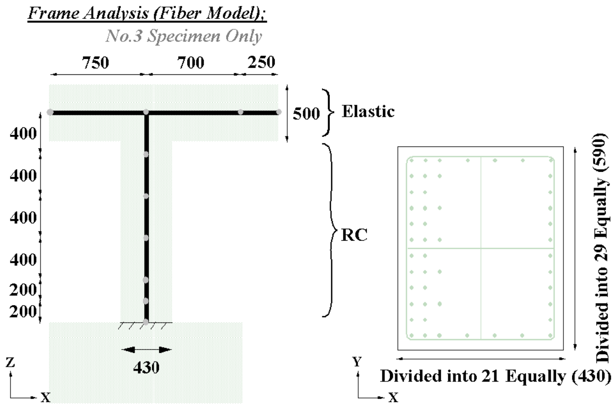

Fig. 14-2 Mesh Definition for Frame Analysis [11]

3.2 Simplified buckling model

The deformability and ductility of RC columns subjected to torque and a bending moment are affected by cover concrete spalling and by reinforcing bar buckling. In RC columns of the scale and dimensions generally used as piers in the Japanese infrastructure, it can be said that the effects of spalling or buckling on a structural member's post-yield capacity are relatively small. The ratios of cover thickness and bar diameter to cross section are relatively smaller in real structures than in small-scale specimens. However, stiffness in unloading and energy absorption are affected by these phenomena, and it is appropriate to consider their influence when repeated loading is under investigation. In order to evaluate the post-peak behavior adequately, it is necessary to incorporate these phenomena into the analytical method.

Full three-dimensional microscopic solid analysis using quite fine elements and considering geometrical nonlinearities may be the most effective solution to this. Swelling of the main reinforcing bars may be treated as a local buckling phenomenon. The basic constitutive models of plain concrete, for example [13], could be applied even to reinforced concrete composites, and tension-stiffening (representing the bond characteristics between concrete and steel) would not have to be taken into account in the elements. In this case, however, the element length must be made as small as the rib size of a deformed bar [16]. Thus, the method is impractical given the present level of computing technology.

On the other hand, spatially averaged equivalent material models for concrete spalling and buckling of reinforcing bar cross-arranged within structures have been proposed [10][17][18]. These allow comparatively coarse elements to be defined for the analysis. The material model proposed by Dhakal et al. [10] is formulated using the length-to-diameter ratio (L/D) and the yield strength of the reinforcing bars as parameters with application to frame analysis based on the fiber technique in mind. The buckling length (L) is determined from the energy equilibrium of axial force and lateral confining force due to the stirrups by assuming a cosine function for the shape of the reinforcing bars after buckling. This is illustrated in Fig. 15 [18]. Consequently, the

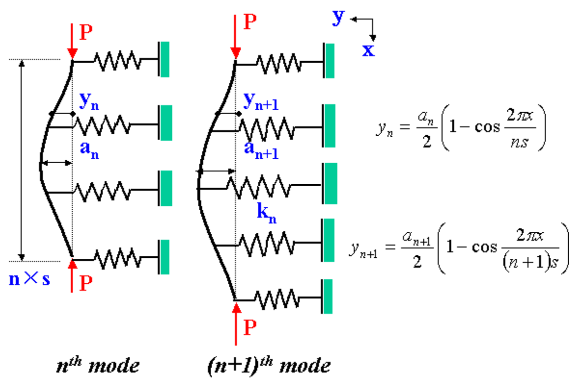

Fig. 15 Outline of Definitive Method of Buckling Length [10][18]

buckling length depends on the bar diameter, bar arrangement and material properties. Moreover, in a case where the assumed buckling length is different from the defined analytical element length, the size effect is taken into account in averaged material models by comparing nonlinearity predominant domain with the unloading domain [22].

Here, this buckling model is selected and transformed for use in full three-dimensional solid analysis. Dhakal et al. directly adopt a material model proposed by Pinto et al. [19] for the hysteresis loop, which is made from loading tests of reinforcing bars as homogenous material. However, this trends to cause an overestimate of energy absorption because the model assumes fixed boundary conditions at each end. Thus, the authors newly define an internal path of lower energy absorption based on previous research in which the material behavior of reinforcing bars in structures was measured [17]. As illustrated in Fig. 16, by dropping the stress inflection point of the Pinto model, the stiffness from compression to tension declines simplistically. This modeling is dealt by considering the stiffness reduction of reinforcing bars inside structures along unloading/reloading path rather than as homogenous steel in which both ends are completely fixed.

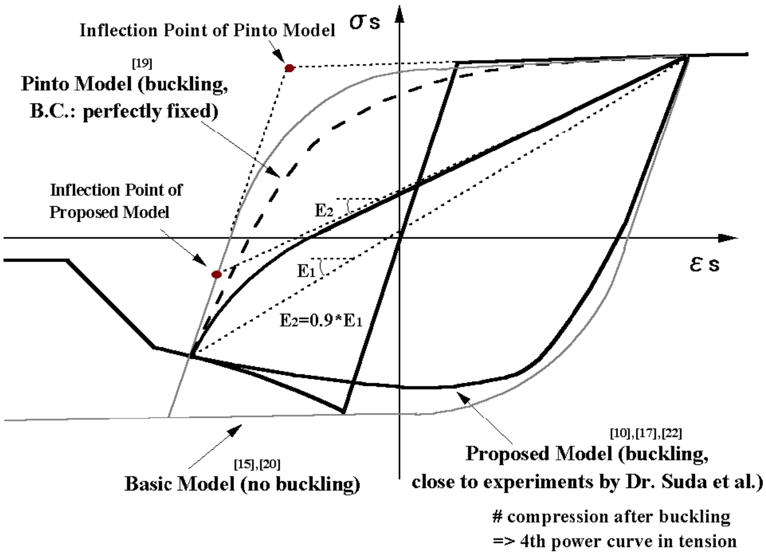

Fig. 16 Summary of Steel Buckling Model Used in Analysis Buckling Length [10]

For specimens1 and 2 subjected to torsion, standard analysis without the buckling model as well as analysis with the proposed buckling model are carried out, and post-peak behavior is also investigated. Although several investigations on the influence of the steel buckling phenomenon on flexural behavior have been reported, little attention has focused on loading paths including torsion. The selected buckling model represents swelling out of reinforcing bars for convenience' sake in static analyses that does not consider local buckling, as explained earlier. Although a rigorous modeling approach that faithfully expresses behavior should be carried out in parallel, the authors are more interested in investigating its degree of influence on structural response. That is, analysis is carried out only using the simplified model in this paper. Although no obvious symptoms of buckling are observed in specimen 2, lateral deformation takes place gradually due to the reversed cyclic loading rather than suddenly. Consequently, analysis with the buckling model is carried out for specimen 2, in which spalling of the cover concrete is observed.

4. ANALYTICAL RESULTS AND CONSIDERATION

4.1 Load versus displacement relationship

The numerical results obtained by full three-dimensional solid analysis are shown in Figs. 3, 4, 6, 7, 8, 10 and 11, superimposed over the experimental values. Results by frame analysis based on the fiber technique are also illustrated for specimen 3. While the authors have published analytical results using a bi-linear model for steel [15] in reference [11], later a tri-linear model for steel in tension, considering the bond effect and the localization of plasticity including rupture, was proposed [20]. Here, simulation using the tri-linear model is once again used and this is presented here.

a) Specimen 1
In the case of standard analysis without the buckling model, the relationship between load and displacement is similar to the experimental result, indicating a flexural response of high ductility and superb energy absorption, as shown in Fig. 3. However, the simulation overestimates the yield capacity slightly, and the discrepancy between experiment and simulation widens gradually as the applied horizontal displacement increases. Stiffness in unloading/reloading is also overestimated as the plasticity ratio in horizontal displacement increases.

The analytical results with the buckling model begin to diverge from the standard ones at 3 δ_y, and conformity with the experimental results is better. The post-yield capacity barely increases in the envelope curve of the load and displacement relationship, and this may indicate that the accuracy of this analysis is better. Focusing on unloading/reloading curve, it can be seen that the stiffness is reduced and a pinch effect appears. Clearly, introduction of the buckling model leads to better representation of stiffness deterioration and energy absorption, and the analytical results are closer to the experimental ones. One as-yet unidentified problem is that the simulation slightly overestimates the yield capacity on the positive loading side. It can be said, however, that analytical accuracy is not a serious concern as long as structural dimensions of specimens and achievements on response analysis of flexure behaviors are taken into consideration. Overall, these results suggest that analysis that takes into account the buckling of reinforcing bars can lead to significant improvements in response analysis of structural behavior in the highly inelastic range.

The initial torque disappears from the relationship between torsional force (difference between reaction forces of the two jacks) and displacement as the flexural deformation increases. This is satisfactorily estimated by the simulation, as shown in Fig. 4. The reason for this disappearance of the initial torque is that crack initiation by bending/shear causes a simultaneous decrease in torsional stiffness. This means that the three-dimensional intersecting effect of torsional/shear diagonal cracks and bending cracks is adequately modeled by solid analysis; frame analysis is fundamentally incapable of achieving this. Incidentally, the effect of the buckling model on torque reduction is barely observed in the analysis.

b) Specimen 2
In the case of standard analysis without the buckling model, even though loading path is the most complex in this case, the simulation is able to estimate the flexure/shear response behavior with a certain accuracy in the relationship between load and displacement, as shown in Fig. 6. Because the initial torque is nearly equal to the steel yielding moment, cover concrete damage is relatively heavy and post-peak behavior appears in the analysis, too. No pinch effect is seen, matching the experimental results. A detailed investigation of the internal stress field shows that the crack plane derived from bending/shear continues to contact somewhere due to the existence of permanent eccentric axial force even in the highly plastic range and, consequently the compressive stiffness in axial direction does not decrease [11]. However, the initial stiffness at 1 δ_y is underestimated in the analysis. Bending capacity and unloading stiffness in the analysis begin to diverge from the experimental values, and the discrepancy gradually increases as the applied horizontal displacement increases, as with specimen 1.

When the buckling model is incorporated into the analysis, difference of hysteresis loop begins to be seen from 1 δ_y and divergence of capacity value from 2 δ_y, thereafter, the discrepancies gradually increases. The capacity reduction becomes significant after 3 δ_y in the envelope curve of the load and displacement relationship. This may indicate that the accuracy of this analysis is better, though the difference between the two analyses is not that great. Along the unloading/reloading path, the unloading stiffness and energy absorption drop significantly and the simulation closely matches the experiment. As with specimen 1, analysis in which reinforcing bar buckling is taken into account contributes to improved estimation in the highly inelastic range.

The initial torque falls, as in the experiment, in the relationship between torsional force and displacement as flexure deformation increases, as shown in Fig. 7. Unlike specimen 1, however, the torsional force remains in the highly inelastic range, and this may be result from the high degree of torsion. Analysis with the buckling model indicates a slightly higher torque reaction as compared to analysis without the buckling model.

The irreversible accumulation of residual displacement in the direction of eccentricity without a horizontal force is clearly expressed in the analysis, as illustrated in Fig. 8. The actual value of the displacement, however, is underestimated. The difference between experiment and analysis initially arises at 1 δ_y, where the damage is not very significant, and is then maintained as the number of loading steps increases. Finally, the differential widens in the highly inelastic range where local damage such as cover concrete spalling and reinforcing bar buckling becomes significant. The initial differential may arise because of local deformation at the base due to large amount of torsion and time-dependent behavior. The latter divergence is more accurately simulated by the analysis when the buckling model is included. The difference between analysis with and without the buckling model begins to appear at 2 δ_y, and the differential gradually widens as the deformation increases.

The simulation still underestimates the residual displacement even when buckling is included, although it is closer to the experimental result. Thus there remains room for improvement in the analytical method. In this analysis, the buckling model is based on the assumption that the steel axis is aligned with the principal compressive stress. It is also well known that cover concrete spalling easily occurs under torque. As a result, it seems reasonable to suppose that the swelling effect of reinforcing bars under torsion may be different from that of those simply subjected to flexural moment.

c) Specimen 3

In line with the experimental results, high-ductility flexural response is seen in the relationship between load and displacement in the horizontal loading direction, as shown in Fig. 10. Frame analysis based on the fiber technique slightly underestimates the yield displacement. The main reason for this may be that the nonlinearity of out-of-plane shear deformation is not taken into account in frame analysis. As a result of attempts to improve the steel model in the highly plastic range, the analysis that includes post-yield bending capacity accords well with the experiment. However, the unloading stiffness is overestimated in the highly inelastic range, and the discrepancy gradually increases. This tendency is more notable in the frame analysis. As with specimen 2, because the crack plane continues to contact somewhere due to the existence of a permanent eccentric axial force and transfers the compressive force, the pinch effect is not seen in the analysis [11].

The accumulation of residual displacement in the direction of eccentricity is seen in both the solid and frame analysis, as illustrated in Fig. 11. The solid analysis accurately reflects the experimental behavior up to the first 5 δ_y cycle. However, while displacement in the direction of eccentricity suddenly increases after the second 5 δ_y cycle in the experiment, the simulation is unable to track this sudden increase. A sudden increase in deformation happens at the same time in the experiment as significant damage to the cover concrete at the base of column. The main reason for the simulation underestimating the residual displacement after the second 5 δ_y cycle may be that spalling and buckling models are not included in the analysis. On the other hand, residual displacement in the direction of eccentricity is somewhat overestimated between 2 δ_y and the first 6 δ_y cycle in the frame analysis. This tendency is particularly notable from 3 δ_y to 5 δ_y. This seems to reflect the influence of the enhanced constitutive model of reinforcing bars [11].

We now want to compare solid and frame analysis based on the fiber technique with degenerated D.O.F. The major differentials in two analyses are dealing with out-of-plane deformation and Euler's assumption that a plane section remains plane. A detailed investigation shows that displacement in the direction of eccentricity begins to diverge at 2 δ_y and then remains constant up to approximately 5 δ_y, before finally diverging further, as indicated in Fig. 11. The frame analysis, which underestimates out-of-plane deformation, overestimates the induced bending moment resulting from applied displacement from the initial stage. As a result, it overestimates the induced main bar stress, too. This may give rise to the differences between the two sets of analytical results between 2 δ_y and 5 δ_y, since the mechanism by which deformation in the direction of eccentricity accumulates have its roots in the complex effects of repeated plasticity of the reinforcing bars under the eccentric axial force.

The fact that the discrepancy increases after the second 5 δ_y cycle may indicate that damage is concentrated around the edges of the cross section and Euler's assumption gradually becomes invalid. The relationship between displacement in the horizontal loading direction and that in the direction of eccentricity progresses in a bow-shape in both experiment and analysis as long as the applied horizontal displacement is small; displacement in the direction of eccentricity is larger when the applied horizontal displacement is small, whereas it becomes smaller when the displacement is large. However, this behavior becomes gradually less significant in the experiment and the solid analysis as the value of applied horizontal displacement increases, and displacement in the direction of eccentricity does not relax when horizontal displacement in the loading direction is applied. In contrast, a clear bow-shape is maintained until the end in the case of frame analysis based on the fiber technique. The reason for this may also be explained by way of Euler's assumption becoming invalid, because a member's stiffness in the direction of eccentricity decreases in the highly inelastic range as the cover concrete spalling and other effects occur.

The analytical results for three specimens have been discussed. The mechanism by which residual displacement in the direction of eccentricity accumulates, as observed in specimens 2 and 3, is not discussed here, because it has previously been reported that complex effects of repeated plasticity of the reinforcing bars under an eccentric axial force may be responsible [11]. However, both analysis and experiment here show that residual displacement accumulates even in specimen 2 when under the same torsion mechanism as specimen 3.

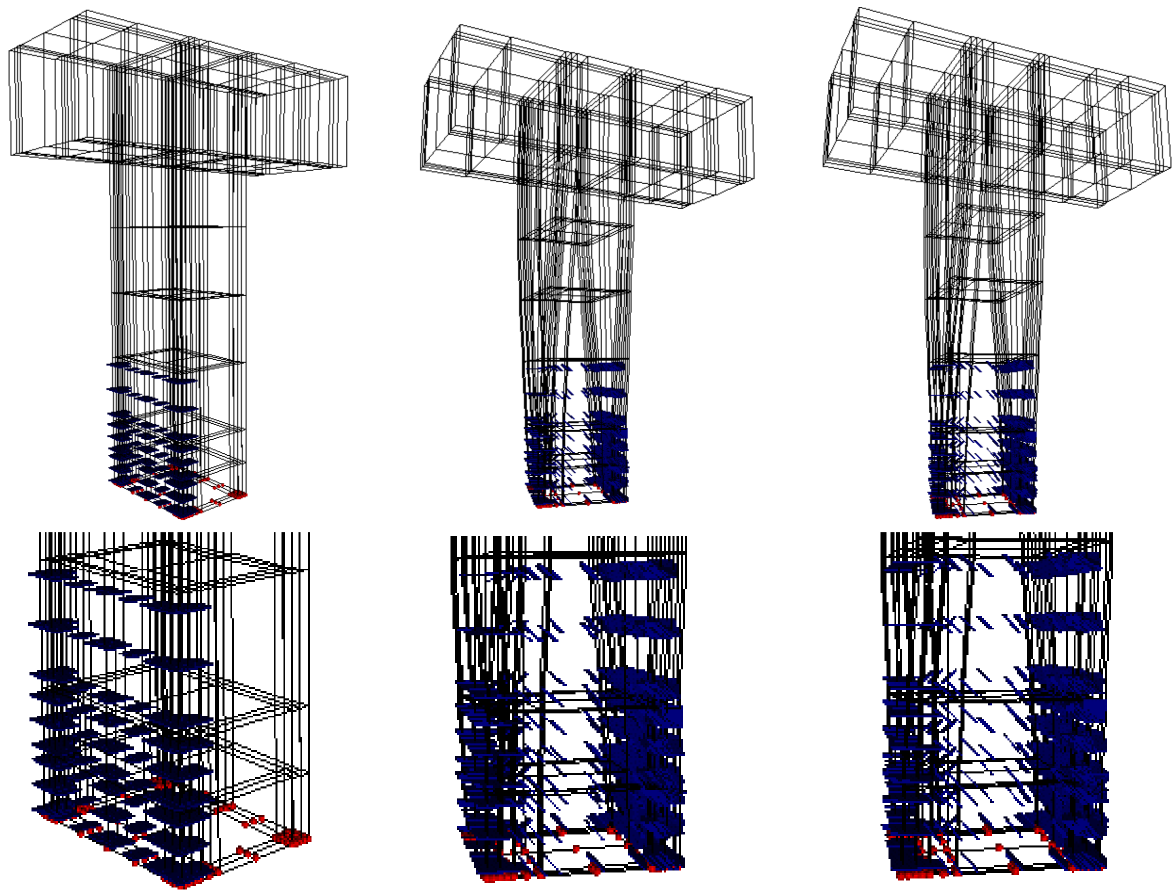

A: Eccentric Axial Force Applied B: Torque Applied C: Bending/Shear Applied

Fig. 17 Crack Drawing in Solid Analysis for Specimens (*upper*; whole structure, *bottom*; enlargement of base)

4.2 Visualization of damage distribution [21]

A schematic representation of the three-dimensional distribution of cracks at certain loading steps is shown in Fig. 17 for specimen 2. This schematic was developed using a method of graphical expression based on the VRML language [21]. Imaginary cracks at each gauss point in the most predominant direction are represented as plates. Although the actual location of a crack with in an analytical element cannot be identified using the analytical method used here, which is founded on a smeared crack approach, the damage distribution can be roughly identified to some degree if the element definition is fine enough.

Figure 17 describes three situations: (A) when the eccentric axial force is initially applied, (B) when torque is applied in the positive direction, and (C) when horizontal force is applied up to +1 δ_y thereafter. It can be seen that horizontal cracking begins at the base of column when bending action occurs due to the eccentric axial force (A). Diagonal cracks are then initiated by torsion (B), and finally deformation progresses by bending/shear (C). However, there is naturally a limit to how well a three-dimensional solid structure can be represented by planes. In particular, at a point where multi-directional cracking in more than three directions is induced in a single element, such as on the side of a column where crack planes induced by reversed cyclic torsion and bending/shear, it is very difficult to realize a solid geometrical shape. The authors are looking for a solution to spatial recognition of the crack distribution. One approach entails "entering" and moving around inside the damaged RC column using an Immersive Multi-Screen Display as used in virtual reality technology [21]. For torsional action, as an example, spirally distributed crack planes can be viewed by "moving" to the center of the member and shifting the viewpoint until it is aligned with the member's axis.

5. CONCLUSIONS

Three-dimensional response analysis of RC column members subjected to a combination of a permanent eccentric axial force, reversed cyclic torsion and bending/shear has been carried out in order to verify the three-dimensional RC constitutive models of a multi-directional fixed crack approach able to consider non-orthogonal cracking. As a result of this work, the following conclusions have been reached:

1) Intersecting cracks in three directions are independently introduced into the target structure, and situation that each cracking plane repeats open/close and shear slip at any locations due to the reversed cyclic action of torsion and bending/shear appears. It is verified that structural analysis based on a non-orthogonal multi-directional fixed crack approach (with a maximum of nine directions in three-dimensional space) is able to estimate the reduction of torque, interaction dependency and loading path of flexural response displacement in two directions, and capacity with adequate accuracy. Because such behavior is closely connected to the effect of intersecting cracks, it appears possible to apply these constitutive models to non-orthogonal independent cracks in three directions at least until the point of deformation at the maximum capacity.

2) It is determined that analytical accuracy can be improved in the post-peak range, where spalling of the cover concrete and swelling of reinforcing bars may occur, by taking into account the large local deformation of the reinforcing bars. It is also supposed that the deterioration of resistant mechanism after steel buckling may be accelerated in the case that torsion and bending/shear force are simultaneously introduced, that means principal stress direction of concrete does not accord with the steel axis direction.

3) The results of three-dimensional frame analysis based on Euler's assumption are compared with solid analysis with no degeneration of D.O.F. This indicates the possibility that response displacement may be underestimated in a case where deformation and damage are concentrated in the corner of a column, because the assumption becomes invalid. Significant concentration of damage appears at the corners of the column base under eccentric axial force and torsion. However, Euler's assumption may be applicable to flexure-prone members up to the neighborhood of their maximum capacity.

Acknowledgements
This research was supported in part by Grant-in-Aid for Scientific Research (No. 11355021) from the Ministry of Education, Culture, Sports, Science and Technology, Japan. The authors wish to express their great gratitude to members of the investigation and research committee of the "Bridge Structures of the Metropolitan Expressway Public Corporation - Concrete Structures Division".

References

[1] Collins, M. and Mitchell, D., "Prestressed Concrete Structures", *Prentice-Hall Inc.*, 1991.
[2] Nagataki, S. et al., "A Study on Mechanism of Torsional Resistance of Reinforced Concrete Members", *Concrete Library International*, No. 12, pp.75-95, JSCE, December 1988.
[3] Fukuura, N. and Maekawa, K., "Spatially Averaged Constitutive Law for RC In-Plane Elements with Non-Orthogonal Cracking as far as 4-Way Directions, *Proc. of JSCE*, No.634/V-45, pp.177-196, November 1999. (in Japanese)
[4] Maekawa, K. and Fukuura, N., "Verification of the Spatially Averaged Constitutive Model with Multi-Directional Cracks on the behavior of RC Structure", *Proc. of JSCE*, No.634/V-45, pp.209-226, November 1999. (in Japanese)
[5] Hauke, B. and Maekawa, K., "Three-Dimensional Modelling of Reinforced Concrete with Multi-Directional Cracking", *Concrete Library International*, No. 36, pp.181-206, JSCE, December 2000.
[6] Maekawa, K., Tsuchiya, S. and Fukuura, N., "Nonlinear Analysis of Reinforced Concrete and Seismic Performance Evaluation", *Proc. of the Second Symposium on Nonlinear Numerical Analysis and its Application to Seismic Design of Steel Structures*, pp.1-16, JSCE, November 1998. (in Japanese)
[7] Masukawa, J., Suda, K. and Maekawa, K., "Three-Dimension Nonlinear FEM Analysis of Hollow Bridge Piers Considering Spalling of Concrete Cover and Buckling of Reinforcing Bars", *Transaction of the Japan Concrete Institute*, Vol. 21, 1999.
[8] Ichikawa, H., Ogasawara, M. and Maekawa, K., "Experimental Study of Seismic Performance of RC Piers Subjected to Eccentric Axial Force and Torsional Moment", *Proc. of* JCI *Symposium on Deterioration of Concrete Members in the Plastic Yielding Stage under Cyclic Seismic Overload*, pp.359-368, August 1998. (in Japanese)
[9] Tsuchiya, S., Ichikawa, H. and Maekawa, K., "Response Analysis of RC Column Subjected to Cyclic Torsion, Shear and Bending", *Proc. of JCI*, Vol.22, No.3, pp.103-108, June 2000. (in Japanese)
[10] Dhakal, R. and Meakawa, K., "Post-Peak Cyclic Behavior and Ductility of Reinforced Concrete Columns", *Seminar on post-peak behavior of RC structures subjected to seismic loads*, Vol.2, pp.151-170, JCI, October 1999.
[11] Tsuchiya, S., Ogasawara, M., Tsuno, K., Ichikawa, H. and Maekawa, K., "Multi-Directional Flexure Behavior and Nonlinear Analysis of RC Columns Subjected to Eccentric Axial Forces", *Concrete Library International*, No.37, pp.1-15, JSCE, June 2001.
[12] Okamura, H. and Maekawa, K., "Nonlinear Analysis and Constitutive Models of Reinforced Concrete", *Gihodo-Shuppan*, May 1991.
[13] An, X., Maekawa, K. and Okamura, K., "Numerical Simulation of Size Effect in Shear Strength of RC Beams", *Concrete Library International*, No.31, pp.323-346, JSCE, June 1998.
[14] Kosaka, H., Ogasawara, M., Sasaki, K., Tsuno, K. Watanabe, E., Tanaka, K. and Sakata, E., "Experimental Study of Seismic Behavior of RC Piers with Various Tie", *Proc. of JCI Symposium on Seismic Retrofitting Techniques for Concrete Structures*, pp.87-96, Apr. 1997. (in Japanese)
[15] Fukuura, N. and Maekawa, K., "Computational Model of Reinforcing Bar under Reversed Cyclic Loading for RC Nonlinear Analysis", *Proc. of JSCE,* No.564/V-35, pp.291-295, May 1997. (in Japanese)
[16] Maekawa, K., An, X. and Tsuchiya, S., "Application to Fracture Analysis of Concrete Structures", *Concrete Journal*, Vol.37, No.9, pp.54-60, JCI, September 1999.
[17] Suda, K. et al., "Buckling Behavior of Longitudinal Reinforcements in RC Column Subjected to Cyclic Load", *Proc. of JCI*, Vol.16, No.2, pp.467-472, 1994 (in Japanese)

[18] Dhakal, R. and Maekawa, K., "Determination of Buckling Length of Reinforcing Bars Based on Stability Analysis", *Proc. of JCI*, No.22, Vol.3, pp.73-78, 2000.
[19] CEB, "RC Elements under Cyclic Loading –State of the Art Report", *Thomas Telford*, 1996.
[20] Hamed, S. and Maekawa, K., "Spatially Averaged Tensile Mechanics for Cracked Concrete and Reinforcement under Highly Inelastic Range", *Concrete Library International*, No.34, pp.151-169, JSCE, December 1999.
[21] Takahashi, T. and Maekawa, K., "Visualization of Three Dimensional RC Crack Analysis Using Immersive Multi-Screen Display", *Proc. of JCI*, Vol.20, No.1, pp.149-154, 1998. (in Japanese)
[22] Dhakal, R. and Maekawa, K., "Post-Peak Cyclic Response Analysis and Energy Dissipation Capacity of RC Columns", *Proc. of JSCE*, No.676/V-51, pp.117-133, May 2001.